RSC Advances

ROYAL SOCIETY OF CHEMISTRY

www.rsc.org/advances

Journal Name

ARTICLE

Effective intensity distribution used for direct laser interference exposure

Jia Xu,[a, b] Zuobin Wang [b, c] , Ziang Zhang [b], Dapeng Wang [b, c] and Zhankun Weng [b]

This paper presents a method to obtain the periodic structures with different feature shapes in direct laser interference lithography. In the method, the desired structures are produced by controlling the effective intensity distributions of interference patterns during the exposure process. The effective intensity distributions are adjusted by changing t - exposure beam intensity based on the material modification thresholds. In the simulations and experiments, the different exposure intensities were used to study the interactions between effective intensity distributions and materials, and the direct four- and six-beam laser interference lithography systems were set up to pattern silicon wafers. The shapes and sizes of the fabricated surface structures were changed with the effective intensities. The experimental results are in accordance with the theoretical models and simulations.

Laser interference lithography is a patterning technology for the fabrication of periodic and quasi- periodic micro and nano structures.[1-3] It has much larger exposure area and deeper exposure field than other lithography technologies, and it has the advantages of low cost and high throughput to fabricate gratings, periodic structured templates, 3D photonic crystals, micro and nano photonic devices and photoelectric sensors.[4-6]

In the process of the traditional laser interference lithography, it utilizes the interference patterns generated by two or more coherent laser beams to obtain the desired surface structures.[7, 8] The technology is developed into a multi-step process.[9,10] The photoresist is used as the sensitive material covered on the sample surface by spin-coating, and then the interference patterns are transferred to the material surface after exposure, development and etching.[11-14] With the development of direct laser interference lithography, the interference patterns based on the high-power laser can be written into the material surface directly without the photoresist and masks to form periodic fringe and dot arrays. It has the advantages of simplicity, high efficiency and 3D patterning compared with the traditional interference lithography.[15-19] In this case, the effective intensity distributions of interference patterns can be used to obtain different shapes of surface structures in an interference system.

In the direct laser interference lithography system, it is assumed that the lithography threshold of the sample is P, and the intensity of the interference pattern is Ps. The effective intensity distribution used to directly modify the sample surface Pe can be expressed as Pe = Ps − P (0< Pe < Ps). Effective intensity distribution is significant for a direct laser interference lithography system, as it is related to the formation of the shapes of surface structures when the wavelength, beam numbers, azimuth angles, incidence angles and polarization directions are selected. The different surface patterns can be obtained by different effective intensity distributions, and the effective intensity distributions can be controlled by adjusting the exposure beam intensity over the material modification threshold.

In this work, we described the theoretical models and simulations of the direct four- and six-beam laser interference, and used the effective intensity distribution of the interference patterns to modify the silicon wafer surface. The desired periodic structures were fabricated directly on the material surface by the proper selection of the interference intensity distribution over the thresholds. The morphology of the exposure structures are characterized by SEM, and the experiment results have shown that the effective intensity distribution of the interference patterns can be used to form the periodic structures with different sizes and shapes in the direct laser interference lithography system.

Theoretical analysis and simulation

The general form of N-beam laser interference can I . described as the superposition of the electric field vectors of N coherent beams. The electric field vector of the n-th beam can be expressed as[20]

$$\vec{E}_n = A_n \vec{p}_n \cos(\vec{k}_n \cdot \vec{r}_n - \omega \cdot t + \varphi_n) \tag{1}$$

a. Changchun Institute of Optics, Fine Mechanics and Physics, Chinese Academy of Sciences, Changchun 130033, China.
b. CNM & JR3CN, Changchun University of Science and Technology, Changchun 130022, China.
c. JR3CN & IRAC, University of Bedfordshire, Luton LU1 3JU, UK.

where A_n is the amplitude, $\vec{p}_n$ is the unit polarization vector, $\vec{k}_n$ is the vector in the propagation direction, $\vec{r}_n$ is the position vector, ω is the frequency and φ_n is the initial phase. In Eq. (1), $\vec{r}_n$, $\vec{p}_n$ and $\vec{k}_n$ can be expressed as

$$\vec{r}_n = x \cdot \vec{a} + y \cdot \vec{b} + z \cdot \vec{c} \tag{2}$$

$$\vec{k}_n = k(\sin\theta_n \cdot \cos\phi_n \cdot \vec{a} + \sin\theta_n \sin\phi_n \ \vec{b} - \cos\theta_n \cdot \vec{c}) \tag{3}$$

$$\vec{p}_n = -(\cos\theta_n \cdot \cos\phi_n \cdot \cos\psi_n - \sin\theta_n \sin\psi_n) \vec{a} - \tag{4}$$

$$(\cos\theta_n \cdot \sin\phi_n \cdot \cos\psi_n + \cos\theta_n \sin\psi_n) \vec{b} - (\sin\phi_n \cdot \cos\psi_n) \vec{c}$$

where $k = 2\pi/\lambda$, $\vec{a}$ is the vector in the x-axis direction, $\vec{b}$ is the vector in the y-axis direction, $\vec{c}$ is the vector in the z-axis direction, λ is the wavelength, θ_n is the incidence angle, ϕ_n is the azimuth angle and ψ_n is the polarization angle. In the N-beam interference field, the intensity distribution can be expressed as

$$I = \sum_{n=1}^{N}\sum_{m=1}^{N} A_n \vec{p}_n \cdot A_m \vec{p}_m \cdot e^{[i(\vec{k}_n - \vec{k}_m)\vec{r} + \phi_n - \phi_m]} \tag{5}$$

In the experiments, the systems of four- and six-beam laser interference lithography are used to obtain the desired interference patterns by fixing the number of beam to four and six. Four-beam laser interference can generate patterns with an array of dots or holes, and six-beam laser interference can generate modulated patterns.

Direct four-beam interference

The scheme of a direct four-beam interference setup is shown in Fig. 1. For the direct four-beam interference, the laser source is divided into four beams with the azimuth angles of $\varphi_1 = 0°$, $\varphi_2 = 90°$, $\varphi_3 = 180°$ and $\varphi_4 = 270°$, and the incidence angles of $\theta_1 = \theta_2 = \theta_3 = \theta_4 = \theta$. It is assumed that the amplitudes of beams are identical. The intensities of interference is expressed as

$$I_{Four-beam} = 2A^2 \left\{ \begin{array}{l} 2 + \cos(2kx\sin\theta) + \cos(2ky\sin\theta) + \\ 2\cos[k(x-y)\sin\theta] + 2\cos[k(x+y)\sin\theta] \end{array} \right\} \tag{6}$$
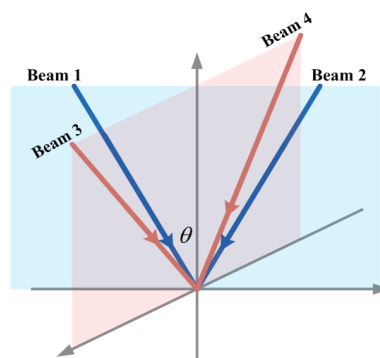

Fig. 1 Direct four-beam interference configurations: beam 1 and beam 2 are in the same incidence plane which is orthogonal to the plane of beam 3 and beam 4.

To study the interaction between the effective intensity distribution and the threshold of the material, the simulation of direct four-beam laser interference exposure is performed to obtain the interference patterns.[21-24] In the simulation, the interference patterns with different effective intensity distribution shapes are obtained, as shown in Fig. 2. With the reduction of the exposure beam intensity over the material modification thresholds, the shape of the periodic patterns are changed gradually during the direct interference exposure, such as periodic hole-arrays, periodic grid-arrays and periodic elliptical dot-arrays.
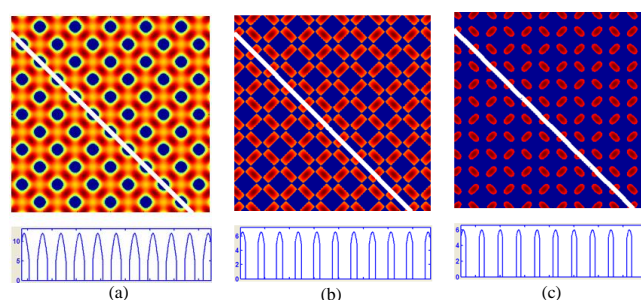

Fig. 2 Effective intensity distributions used for direct four-beam interference with reduced exposure beam intensities: (a) periodic hole-arrays; (b) periodic grid-arrays; (c) periodic elliptical dot-arrays.

Direct six-beam interference exposures

The moth-eye structures have the unique feature for a high absorption of the incidence light due to the dual structure distribution on the surface. [25-28] To obtain the structures similar to moth eyes, the effective intensity distribution used for direct six-beam laser interference is designed to fabricate moth-eye-like dual structures.
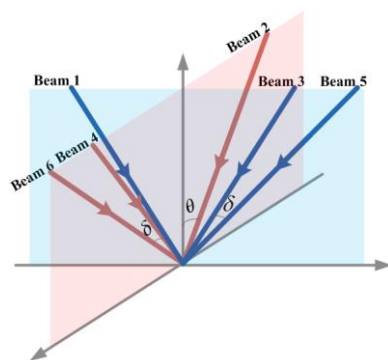
Fig. 3 Direct six-beam interference configuration: Beam 1, beam 3 and beam 5 are in the same incidence plane which is orthogonal to the plane of beam 2, beam 4 and beam 6.

Compared with six azimuth angles, the configuration of four azimuth angles has the advantage of good controllability regarding the pattern structures in the direct six-beam interference lithography system. As shown in Fig. 1, the six incidence beams follow a configuration with the azimuth angles of $\varphi_1 = 0°$, $\varphi_3 = \varphi_5 = 180°$, $\varphi_2 = 270°$ and $\varphi_2 = \varphi_4 = 90°$. The incidence angles of the six beams can be set as $\theta_1 = \theta_2 = \theta_3 = \theta_4 = \theta$ and $\theta_5 = \theta_6 = \theta + \delta$. It is assumed that the amplitudes of the six beams are identical and the initial phases are zero. According to Eq. (5), the intensity distribution of the six-beam interference field can be calculated by

$$I = 2A^2 \left\{ \begin{array}{l} 3 - \cos(2k\sin\theta \cdot x) + \cos\left\{ \begin{array}{l} [\sin\theta - \sin(\theta+\delta)]x \\ -[\cos\theta - \cos(\theta+\delta)]z \end{array} \right\} \\ -\cos\left\{ \begin{array}{l} [\sin\theta + \sin(\theta+\delta)]x + \\ [\cos\theta - \cos(\theta+\delta)]z \end{array} \right\} \\ -\cos(2k\sin\theta \cdot y) + \cos\left\{ \begin{array}{l} [\sin\theta - \sin(\theta+\delta)]y \\ -[\cos\theta - \cos(\theta+\delta)]z \end{array} \right\} \\ -\cos\left\{ \begin{array}{l} [\sin\theta + \sin(\theta+\delta)]y + \\ [\cos\theta - \cos(\theta+\delta)]z \end{array} \right\} \end{array} \right\} \quad (7)$$

As shown in Figs. 4(a)-(c), the dual structures are obtained with the reduction of effective intensity distributions during direct six-beam interference simulations. The desired periodic dot structures can be fabricated by the proper selection of the interference intensity distribution over the thresholds.
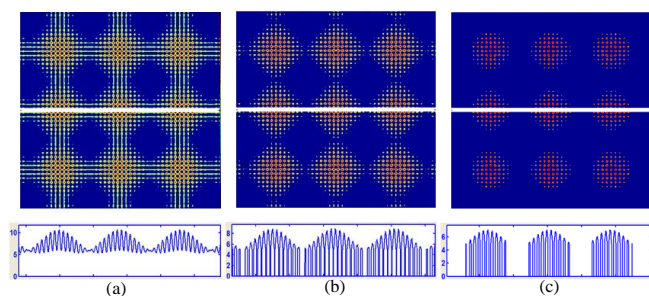

(a) (b) (c)

Fig. 4 Effective intensity distributions used for the formation of dual structures in direct six-beam interference.

Experiment

The interaction process between the intensity distribution of interference pattern and the silicon surface is the excitation of the electrons from the equilibrium states to the excited states by the absorption of photons, as shown schematically in Fig. 5. In the exposure process of direct laser interference lithography, the electrons are excited from the valence band to the conduction band by the absorption of photons. It is known that for a given interference pattern the effective intensity distribution introduces the subsequent processes including melting, boiling and ablation of silicon. In this method, the smallest size that we have obtained using this method is about 20 nm.
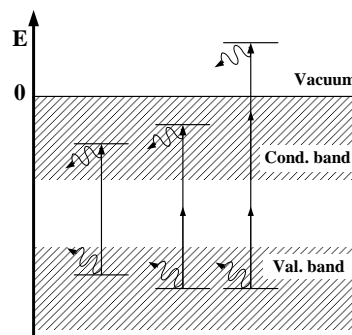

Fig. 5 Primary electronic excitation in semiconductors by absorption of photons.

In the experiments, four- and six-beam interference lithography systems were set up. As shown in Fig. 6, the pulsed Nd:YAG laser with the wavelength of 1064 nm, laser fluence of about 1800 mJ/cm^2, exposure frequency of 10 Hz, beam diameter of 9 mm and pulse duration of 6-8 ns was used as the system light source. The laser beam was split into four and six beams by beam splitters B1-B5. The incidence angle and azimuth angle of each beam were adjusted by controlling the position of mirrors M1-M5. The half-wave plates H1-H6 and polarizers P1-P6 were used to select polarization directions and exposure intensities for each beam before the beams interfered on the sample wafer surface. The samples used in the exposure were polished single crystal P-doped silicon wafers, and all the processes were carried out under clean-room conditions.
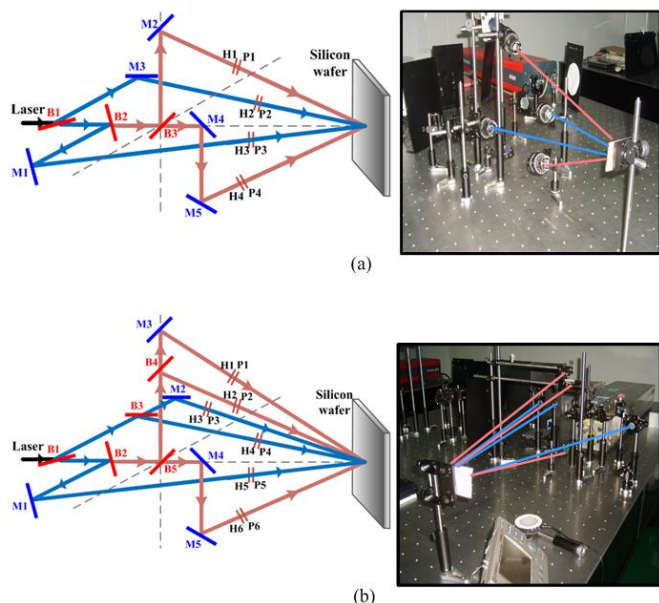
(a)

(b)

Fig. 6 Schematic and real set-ups for (a) four-beam laser interference; (b) six-beam laser interference. M1-M5 are the high-reflective mirrors, B1-B5 are the beam-splitters, H1-H6 are the half wave plates and P1-P6 are the polarizers.

Results and discussions

In the experiment of direct four-beam interference lithography, the laser source was divided into four beams with the azimuth angles of $\varphi_1 = 0°$, $\varphi_2 = 90°$, $\varphi_3 = 180°$ and $\varphi_4 = 270°$. The four coherent beams were incident on the sample surface with the identical incidence angles of $\theta = 5°$. The laser fluence was about 640 mJ/cm^2 for 60s. Because of the non-flat intensity distribution of the laser spot, the structures based on different effective intensity distributions were obtained from the centre to the edge of the spot. Figs. 7(a) and (b) show the SEM micrographs of the periodic structures of direct four-beam interference with the reduced exposure beam intensity over the material modification thresholds. As shown in Fig. 7(a), the periodic hole-arrays were formed due to the stronger power of the spot centre. Fig. 7(b) shows the periodic grid-arrays and elliptical dot-arrays formed in the area located on the spot edge. Figs. 8(a) and (b) show the cross-sectional views (Carl Zeiss Axio CSM 700 confocal microscope) of the periodic structures fabricated by direct four-beam interference with the reduced exposure beam intensity over the material modification thresholds.
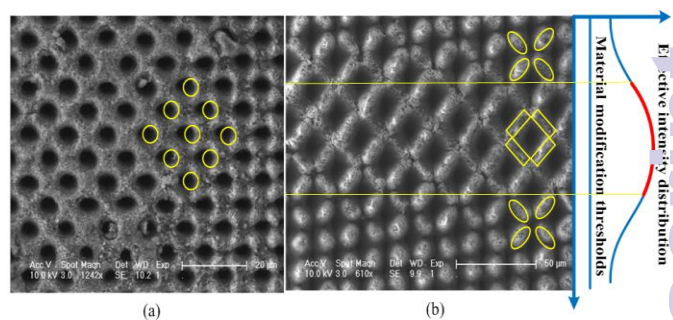

Fig. 7 SEM micrographs of the periodic structures fabricated by direct four-beam interference with the reduced exposure beam intensity over the material modification thresholds: (a) periodic hole-arrays; (b) periodic grid-arrays and periodic elliptical dot-arrays.
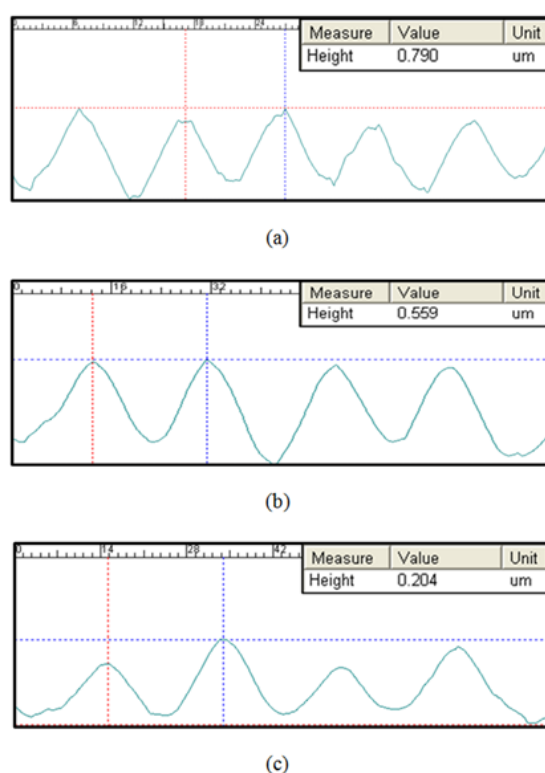

Fig. 8 Cross-sectional views of the periodic structures fabricated by direct four-beam interference with the reduced exposure beam intensity: (a) periodic hole-arrays; (b) and (c) periodic grid-arrays and periodic elliptical dot-arrays.

In the process of direct six-beam interference exposure, the laser beam was divided into six beams with the azimuth angles of $\varphi_1 = 0°$ $\varphi_3 = \varphi_5 = 180°$, $\varphi_2 = 270°$ and $\varphi_2 = \varphi_4 = 90°$. The incidence angles of the six beams were set as $\theta_1 = \theta_2 = \theta_3 = \theta_4 = \theta = 7°$. Six half wave plates and six polarizers were placed in pairs before the six interfering beams to obtain TE coherent beams and adjust the exposure intensities. Different exposure doses were used to determine the optimum dose for the desired patterns. In this case, the results were achieved with the pulse energy density of 0

Journal Name

ARTICLE

mJ/cm^2，22 mJ/cm^2 and 15 mJ/cm^2, as shown in Figs. 9(a)-9(c). The cross-sectional views of the periodic structures fabricated by direct six-beam interference with the different exposure intensities are shown in Fig. 10.
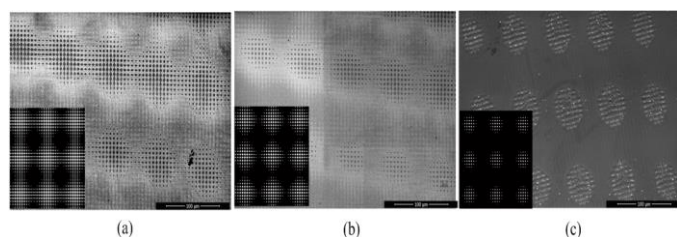

Fig. 9 SEM micrographs of the dual structures with different exposure intensities: (a) pulse energy density of 30 mJ/cm^2; (b) pulse energy density of 22 mJ/cm^2; (c) pulse energy density of 15 mJ/cm^2.
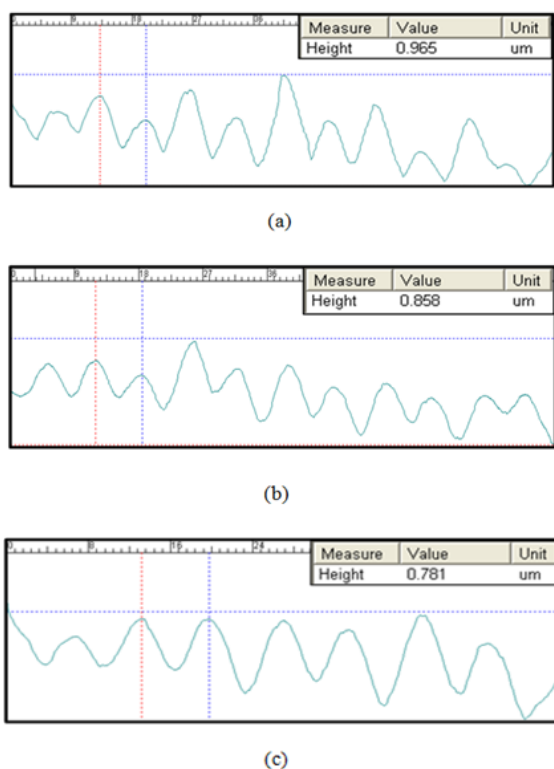

Fig. 10 Cross-sectional views of the dual structures fabricated by direct six-beam interference with different exposure intensities: (a) pulse energy density of 30 mJ/cm^2; (b) pulse energy density of 22 mJ/cm^2; (c) pulse energy density of 15 mJ/cm^2.

Conclusion

In this work, a method to obtain the periodic structures with different feature shapes has been presented and examined in direct laser interference lithography. The method features the control of the effective intensity distributions used for the fabrication of periodic surface structures.

The effective intensity distributions can be controlled by changing the exposure intensity based on the material modification thresholds during the exposure process. The results of simulations and experiments achieved by direct four- and six-beam laser interference have shown that the desired periodic structures can be fabricated directly on the silicon surface by the proper selection of the effective intensity distributions of the interference patterns. There is a good correspondence between the resulting structures and the theoretical models and simulations.

References

1. Q. Xie, M. H. Hong, H. L. Tan, G. X. Chen, L. P. Shi, and T. C. Chong, J. Alloys Compd. 449, 261 (2008).
2. L. F. Johnson, G. W. Kammlott, and K. A. Ingersoll, Appl. Opt. 17, 1165 (1978).
3. Z. Wang, J. Zhang, C. S. Peng and C. Tan, in Proceedings of IEEE Conference on Mechatronics and Automation (Institute of Electrical and Electronics Engineers, Harbin, 2007), pp. 434-439.
4. Y. F. Liu, J. Feng, Y. G. Bai, J. F. Song, Y. Jin, Q. D. Chen, H. B. Sun, Opt. Lett. 37, 124 (2012).
5. X. Zhang, J. Feng, J. Song, X. Li, H. Sun, Opt. Lett. 36, 3915 (2011).
6. D. D. Zhang, J. Feng, H. Wang, Y. F. Liu, L. Chen, Y. Jin, Y. Q. Song, Y. Bai, Q.D.Chen, H.B. Sun, IEEE. Photonics. J. 3, 26 (2011).
7. S. R. J. Brueck, in Proceedings of Institute of Electrical and Electronics Engineers. (New Mexico University, Albuquerque, 2005), pp. 1704-1721.
8. J. Xu, Z. Wang, Z. Weng, Z. Li, X. Sun, L. Liu, L. Zhao, Y. Yue and J. Zhang, Key Eng. Mater. 552, 262 (2013).
9. N. D. Lai, W. p. Liang, J. H. Lin, C. C. Hsu, and C. H. Lin, Opt. Lett. 13, 9605 (2005).
10. J. H. Moon and S. Yang, J. Macromol. Sci. Polym. Rev. 45, 351 (2005).
11. J. H, Z. Moon, J. Ford, and S. Yang, Polym. Adv. Technol. 17, 83 (2006).
12. S. Z. Su, A. Rodriguez, S. M. Olaizola, C. S. Peng, C. Tan, Y. K. Verevkin, T. Berthoud and S. Tisserand, Proc. SPIE. 65930G, pp. 1-8 (2007).
13. C. G. Chen, R. K. Heilmann, C. Joo, P. T. Konkola, G. S. Pati, and M. L. Schattenburg, J. Vac. Sci. Technol. B 20, 3071 (2002).
14. C. P. Fucetola, H. Korre and K. K. Berggren, J. Vac. Sci. Technol. B 27, 2958 (2009).
15. M. Ellman, A. Rodríguez, N. Pérez, M. Echeverria, Y. K. Verevkin, C. S. Peng, T. Berthou, Z. Wang, S. M. Olaizola, and I. Ayerdi, Appl. Surf. Sci. 255, 5537(2009).
16. W. Zhao, J. Li, H. K. Kang, B. Zhou, C. C. Wong, Nanosci. Nanotech. Let. 3, 246 (2011).
17. A. F. Lasagni, D. F. Acevedo, C. A. Barbero and F. Mucklich, Adv. Eng. Mater. 9, 99 (2007).
18. Y. Zabila, M. Perzanowski, A. Dobrowolska, M. Kac, A. Polit and M. Marszalek, Acta Phys. Pol., A 115, 591 (2008).
19. D. A. Acevedo, A. F. Lasagin, C. A. Barbero and F. Mücklich, Adv. Mater. 19, 1272 (2007).
20. J. Zhang, Z. Wang, Y. K. Verevkin, S. M. Olaizola, C. Peng, C. Tan, A. Rodriguez, E. Y. Daume, T. Berthou, S. Tisserand and Z. Ji, in Proc. SPIE 6593, Photonic Materials, Devices, and Applications II (Maspalomas, Gran Canaria, Spain, 2007), pp1-8.
21. C. Tan, C. S. Peng, J. Pakarinen, M. Pessa, V. N. Petryakov, Y. K.Verevkin, J. Zhang, Z. Wang, S. M. Olaizola, T. Berthou and S. Tisserand, Nanotechnology 20, 125303 (2009).
22. R. Guo, D. Yuan, S. Das, J. Micromech. Microeng. 21, 1501 1 (2011).
23. T. Tavera, N. Pérez, A. Rodríguez, P. Yurrita, S.M. Olaizola, E. Castano, Appl. Surf. Sci. 258, 1175 (2011).
24. D. Wang, Z. Wang, Z. Zhang, Y. Yue, D. Li, and C. Maple, Appl. Surf. Sci. 282, 67 (2013).

25. R. Murillo, H. A. Wolferen, L. Abelmann, and J. C. Lodder, Miner. Eng. 78–79, 260 (2005).
26. L. Wang, B. B. Xu, Q. D. Chen, Z. C. Ma, R. Zhang, Q. X. Liu, and H. B. Sun, Opt. Lett. 36, 3305 (2011).
27. K. M. Baker, Appl. Opt. 38, 352 (1999).
28. J. Xu, Z. Wang, Z. Zhang, D. Wang and Z. Weng, J. Appl. Phys. 115, 203101 (2014).

RSC Advances Accepted Manuscript